Journal of Molecular Liquids 172 (2012) 110–118

Contents lists available at SciVerse ScienceDirect

Journal of Molecular Liquids

journal homepage: www.elsevier.com/locate/molliq

From microhydration to bulk hydration of Sr^{2+} metal ion: DFT, MP2 and molecular dynamics study

Anil Boda [a], Sulagna De [b], Sk. Musharaf Ali [a,*], Srinivas Tulishetti [c], Sandip Khan [c], Jayant K. Singh [c,**]

[a] Chemical Engineering Division, Bhabha Atomic Research Centre, Mumbai, 400085, India
[b] Radioactive Ion Beam Group (RIBG), Variable Energy Cyclotron Centre (VECC), Kolkata, 700064, India
[c] Department of Chemical Engineering, Indian Institute of Technology Kanpur, Kanpur, 208016, India

ARTICLE INFO

Article history:
Received 7 March 2012
Received in revised form 4 April 2012
Accepted 2 May 2012
Available online 25 May 2012

Keywords:
Microhydration
Strontium
DFT
MP2
MD
EXAFS

ABSTRACT

This paper presents the results of quantum chemical and classical molecular dynamics (MD) simulations of the microhydration states of the Sr^{2+} ion. The quantum chemical results strongly suggest a coordination number (CN) of 8 for the first hydration shell of Sr^{2+}, which is in quantitative agreement with data available from X-ray absorption fine structure (XAFS) measurements. The calculated theoretical Sr – O bond distance of 2.59 Å is also in excellent agreement with the XAFS results (2.60 Å). Classical MD simulations are conducted on various water models to predict the hydration structure of the Sr^{2+} ion. The CN is found to be in the range of 8–9 using SPC, TIP3P, and TIP4P-2005 water models, with the probability more skewed toward 8. MD–EXAFS study and coordination number analyses reveal that TIP4P-2005 is the best model potential for simulating water molecules to reproduce the experimentally observed absorption spectra and coordination numbers.

1. Introduction

An understanding of quantitative metal ion–ligand binding properties is of immense importance in the diverse fields of chemistry, physics, and biology, as well as in the technological developments of various practical separation processes [1–15]. Stepwise addition of ligand molecules to bare metal ions in the gas phase yields coordination complexes. In the case where the ligand molecule is water, the solvation of the metal ion due to successive addition of water molecules is commonly known as microhydration. When a positively charged metal ion is immersed into a purely aqueous solvent pool, the hydrogen-bonded network of water is modified to accommodate the ionic species in the process of hydration. Thus, a delicate balance between cation–water and water–water interactions determines the structure of the hydrated clusters of the cation. The number of water molecules that are directly linked to the metal ion determines its coordination number. Filling of the first coordination shell is succeeded by hydrogen bonding of incoming water molecules to those in the first coordination shell, leading to a hydrated ion cluster. ^{90}Sr, in conjunction with Cs, is one of the major sources of heat generation in aqueous nuclear waste. Hence, separation of ^{90}Sr from the nuclear waste prior to vitrification is mandatory. Sr also has other commercial and research values including its use in certain optical materials, as an oxygen eliminator in electron tubes, and to produce glass for color television tubes. In addition, ^{90}Sr has been used as an isotopic energy source in various research applications. The daughter product of ^{90}Sr decay (^{90}Y) is used as a useful radioisotope in nuclear medicine.

Thus, separation of the Sr metal ion is necessary not only for nuclear waste management but also for its other useful applications. Recently, the use of crown ethers has become very popular for the extraction of alkali and alkaline earth metal ions due to the high selectivity of these ligands for particular metal ions, which are usually present in aqueous solution. During the metal ion–crown ether interaction, the metal ion is transferred from the aqueous phase and is encapsulated in the cavity of the crown ether with the help of weak coordinate covalent bonds. Because Sr^{2+} is mainly present in aqueous phases, knowledge of the coordination number and binding enthalpies of $Sr^{2+}-(H_2O)_n$ clusters are potentially useful for these extraction studies. Such investigations can be conducted by means of experimental techniques or theoretical methods such as quantum mechanics/molecular modeling QM/MM, molecular dynamics (MD), or Monte Carlo (MC).

Several gas phase ionization techniques have been used to predict the metal ion solvation shell size from the sequential binding enthalpies of the hydrated metal ion cluster [16–25]. Vibrational spectroscopy [2,26] has also been used to predict the infrared spectra of mass-selected hydrated cluster ions and hence facilitate the understanding of the underlying mechanism of filling of the solvent shells and formation of hydrogen bonds. These small finite systems offer a number of advantages over traditional solution-based measurements,

* Corresponding author. Tel.: +91 22 25591992; fax: +91 22 25505151.
** Corresponding author. Tel.: +91 512 2596141; fax: +91 512 2590104.
E-mail addresses: musharaf@barc.gov.in (S.M. Ali), jayantks@iitk.ac.in (J.K. Singh).

0167-7322/$ – see front matter © 2012 Elsevier B.V. All rights reserved.
doi:10.1016/j.molliq.2012.05.006

and perhaps are the most useful way to evaluate the veracity of current theoretical calculations and models. Thermodynamic properties derived from high-pressure mass spectrometry measurements may offer an indication of the solvation shell size, whereas vibrational spectra suggest a more complex microscopic picture. A wide range of empirically derived Sr^{2+}–O distances varying from 2.56 to 2.69 Å, as well as coordination numbers varying from 7 to 10.3 have been reported in various studies [27–38]. Predictions based on theoretical calculations engender an equivalent amount of ambiguity. Classical [39,40] and Car-Parrinello [41] MD simulations also predicted widely spread values for the Sr^{2+}–O distance, ranging from ~2.60 Å to 2.65 Å, and coordination numbers ranging from ~7 to 10. Recently, one study reported the value of the Sr^{2+}–O distance to be 2.69 Å and the first shell coordination number to be 8 based on QM/MM [42] analysis.

Although extensive computational analyses of the structure and energetic aspects of hydrated clusters of smaller alkali metal cations [49–64] have been executed, studies on the hydration cluster of the Sr^{2+} ion remain sparse, and those that have been performed have employed a very small number of water molecules (up to n = 6 only), which is clearly insufficient to generate a correct representation of the coordination structure and energetics. Glendening and Feller [56] performed geometry optimizations and single point energy calculations on $Sr^{2+}-(H_2O)_n$ complexes, for n = 1–6. Klobukowski [60], Bauschlicher and co-workers [51], as well as Kaupp and Schleye [59] determined the binding energies of the hydrated Sr^{2+} ion with n = 1–4, n = 1–3, and n = 1–2 water molecules, using a variety of basis sets. Recently, the binding enthalpy of $Sr^{2+}-(H_2O)_n$ complexes (n = 1–6) has been reported using multiple levels of theory and different basis sets including two different effective core potentials for Sr [32]. The structural properties of the hydrated metal ion system can also be predicted by using experimental techniques such as extended X-ray absorption fine structure (EXAFS) spectral analysis [33]. MD simulations may also be used to model the EXAFS spectra, a technique generally known as MD–EXAFS [39,43–48] analysis.

Taking into account of all these experimental and theoretical investigations, it is evident that the hydration structure of the Sr^{2+} ion remains an unresolved issue, and thus an interesting challenge requiring new experimental and theoretical approaches. On this basis, the gas phase hydration study of $Sr^{2+}-(H_2O)_n$ was undertaken in this study, and the structures (coordination number), energetics, and thermodynamic parameters were calculated for a large number of hydrated clusters up to n = 24 using n = m1 + m2 + m3, where m1, m2, and m3 represent the number of water molecules in the first, second, and third solvation shells, respectively. This study is anticipated to enrich the existing knowledge base by furnishing data on molecular level interactions between solvent water molecules and bi-valent ions in aqueous solution. These studies on the size selected hydrated metal ion clusters also play a critical role in facilitating the understanding of the evolution of molecular properties based on the number of solvent water molecules present in the cluster, and to bridge the gap between monohydrated clusters and the hydrated metal ion in bulk aqueous solution. In addition, this study also addresses the question of the accuracy of coordination number calculations from classical molecular dynamics simulations based on the different water models [65–71] such as SPC, TIP3P, and TIP4P-2005. To address this issue, MD–EXAFS analysis of the aqueous strontium (Sr^{2+}) ion was also performed using various water models such as SPC, TIP3P, and TIP4P-2005. The MD–EXAFS results are compared with the available experimental results [33] and a discussion of the data conformity is presented herein.

2. Computational methodology

2.1. Quantum-based modeling

Geometry optimizations of the $Sr^{2+}-(H_2O)_n$ clusters were performed at density functional and MP2 levels of theory. The structural and thermodynamic properties of the hydrated strontium ion clusters were determined with the quantum chemical hybrid density functional (Becke's three parameter non-local hybrid exchange correlation functional), namely B3LYP [72,73], using the cc-PVDZ basis functions for H and O, and the split valence 3–21 G basis function for Sr. The optimized structures were further re-optimized at the MP2 level of theory [74] to study the effect of electron correlation on the calculated structures and energetics. The consideration of the 3–21 G basis set for the Sr^{2+} metal ion did not introduce significant error in the energetics, as was determined by a separate check using the extended LAN2DZ basis set (obtained from the EMSL basis set exchange library) for the Sr metal ion at both the DFT and MP2 levels of theory (discussed later). In the present calculations, several possible starting geometries were empirically generated based on the different possible intermolecular interactions in the $Sr^{2+}-(H_2O)_n$ clusters, n = 1–24. Subsequent to the formation of the mono-hydrated $Sr^{2+}-(H_2O)$ complex, the incoming water molecule may become linked to the existing cluster by two possible means. It may be directly bound either to the metal ion or to the water molecule, via hydrogen bonding. Hence, to determine a stable equilibrium structure for the $Sr^{2+}-(H_2O)_n$ cluster, various possible geometries were considered as the initially assumed structure followed by full geometry optimizations based on the Newton–Raphson optimization procedure as implemented in the GAMESS electronic structure calculation program [75]. No symmetry restriction was imposed in the adopted optimization procedure. The true stationary structures were assured for all of the optimized equilibrium structures through Hessian calculations at 298.15 K. Hessian calculations were also used for estimation of the thermodynamic parameters. The MOLDEN graphics program was used for the visual representation of various molecular geometries and associated structural parameters [76].

The standard procedure for obtaining the hydration energies of a metal–ligand system is based on the following cluster formation reaction:

$$Sr^{2+} + nH_2O \rightarrow Sr^{2+}-(H_2O)_n. \quad (1)$$

The interaction energy, E^{int}, of these metal-hydrate clusters is defined by the following relation:

$$E^{int} = E_{Sr^{2+}-(H_2O)_n} - \left(E_{Sr^{2+}} + E_{(H_2O)_n}\right) \quad (2)$$

where $E_{Sr^{2+}-(H_2O)n}$ refers to the energy of the $Sr^{2+}-(H_2O)_n$ cluster; $E_{Sr^{2+}}$ and $E_{(H_2O)n}$ refer to the energy of the Sr^{2+} ion and the $(H_2O)_n$ system, respectively. The energy of the $(H_2O)_n$ system is calculated by removing the Sr^{2+} ion from the optimized geometry of that cluster followed by single point energy calculation at the same level of theory.

The hydration energy, E^{hyd}, for the $Sr^{2+}-(H_2O)_n$ hydrated cluster is commonly defined as

$$E^{hyd} = E_{Sr^{2+}-(H_2O)n} - \left(E_{Sr^{2+}} + nE_{(H_2O)}\right), \quad (3)$$

where $E(H_2O)$ refers to the energy of a single H_2O molecule.

Thermal correction of the electronic energy of the optimized hydrated cluster has been performed to predict the thermodynamic parameters [77]. The thermal and zero point energy corrected interaction energy is defined as

$$U^{int} = U_{Sr^{2+}-(H_2O)_n} - \left(U_{Sr^{2+}} + U_{(H_2O)_n}\right), \quad (4)$$

where $U_{Sr^{2+}-(H_2O)n}$, $U_{Sr^{2+}}$ and $U_{(H_2O)n}$ represent the internal energy of the $Sr^{2+}-(H_2O)_n$ cluster, Sr^{2+} ion, and $(H_2O)_n$ system, respectively. The interaction enthalpy (H^{int}) and free energy (G^{int}) for the hydrated

cluster of Eq. (1) are calculated using the following standard thermodynamic relations:

$$H = U + \Delta nRT. \quad (5)$$

$$G = H - T\Delta S. \quad (6)$$

A similar approach was adopted in the case of the hydration enthalpy and hydration free energy using Eq. (3).

2.2. Classical molecular dynamics

MD simulations were performed on the hydrated Sr^{2+} ion using the LAMMPS package [78] by employing the SPC, TIP3P, and TIP4P-2005 water potentials in the NPT ensemble to study the hydration structure and CN of the Sr^{2+} metal ion. Simulations were carried out at a constant temperature of 300 K and pressure of 1 atm, using 511 water molecules, one Sr^{2+} ion, and two chloride ions (in certain cases) to provide a density of 0.99145 g/cm^3. A spherical cutoff of 11 Å was employed to account for all pair interactions. The particle–particle and particle–mesh (PPPM) method was applied to account for the long-range columbic interactions. All simulations were carried out for a total time of 1 ns using a time increment of 1 fs. Lastly, a total time of 200 ps was used to calculate the radial distribution functions at the interval of 10 fs. The coordination number was estimated by integrating the average radial distribution function.

Simulations of the EXAFS spectra for the $Sr^{2+} + 2Cl^- + 253$ water molecule system (for different models) were performed using the MD–EXAFS procedure [39]. Geometry minimization was performed for 100 ps followed by a 200 ps run in the micro-canonical ensemble (NVE) at 300 K and 1 atm using a cut-off distance of 8.5 Å. Thereafter, the NPT ensemble was employed for an additional equilibration run of 1.0 ns followed by a 200 ps production run. The $Sr^{2+}-O$ cluster was generated from the multiple configurations during the production run. Because the inter-atomic distance between the Sr^{2+} ion and the O atom is 2.62 Å [33], a radial distance cutoff of 5.0 Å was employed for the cluster generation. The FEFF [79] and FEFFIT [80] algorithms were used in the estimation of the theoretical EXAFS calculation. These two algorithms are in-built programs in the Artemis [81]/iFEFFIT [82] package. The X-ray scattering on the neighboring oxygen atoms can be represented by the multiple paths from the strontium ion to oxygen atoms using the Artemis program. Each path can be assigned an individual structural parameter [44] (χ) in reciprocal space (k-space), which are used to calculate the mean structural parameter ($\overline{\chi}$). The real space EXAFS spectra were obtained after Fourier transformation of the structural parameter using the FEFFIT [80] algorithm as implemented in the Artemis software and can be written as

$$\overline{\chi}(R) = \frac{1}{\sqrt{2\pi}} \int_0^\infty k^2 \overline{\chi}(k) w(k) e^{i2R} dk \quad (7)$$

where $w(k)$ is the Hanning window [83].

3. Results and discussion

Extensive calculations were carried out using the DFT and MP2 levels of theory to obtain the optimized geometries, interaction/hydration energies, and enthalpies for the hydrated cluster of the Sr metal ion up to n = 24 water molecules. The detailed structural analysis is presented below.

3.1. Structure

The minimum energy structure obtained for the hydrated strontium ion in clusters of various sizes through the optimization based on the total electronic energy is presented in Fig. S1 (Supplementary information). The calculated metal oxygen (M–O) distances for the most stable hydrated strontium ion cluster structures are given in Table 1. The average Sr–O bond distance is lengthened as the size of the cluster increases with the successive addition of water molecules. The detailed structural analysis of the clusters up to n = 7 water units is reported in the Supplementary information.

In the case of the octa-hydrated $Sr^{2+}-(H_2O)_8$ cluster, six minimum energy conformers were predicted. Among these conformers, the structure labeled VIII-a in Fig. 1, in which six water molecules are directly coordinated to the Sr ion in an octahedral fashion, is the most stable. The remaining two water molecules are indirectly coordinated by four hydrogen bonds to give an overall 6 + 2 configuration. The energy difference between the most stable structure and the least stable structure was 23.51 kcal/mol. A hydrated structure with eight water molecules in the first solvation shell, without any hydrogen bonding (8 + 0) was also predicted, displayed as VIII-b in Fig. 1. This structure was less stable than VIII-a (the most stable structure) by 4.66 kcal/mol. Thus, in the case of the octa-hydrated $Sr^{2+}-(H_2O)_8$ cluster (Fig. 1), it was found that the hydrogen bonded isomer (VIII-a) is more stable than the isomer with no hydrogen bonding (VIII-b), which indicates that the water–water hydrogen bonding interaction is dominant over the metal ion–water interaction.

The most stable structure obtained for the nona-hydrate $Sr^{2+}-(H_2O)_9$ cluster is also presented; three minimum energy structures were predicted in this instance. In this case, the most stable structure (IX-a, Fig. 1) is the 6 + 3 configuration in which the Sr^{2+} metal ion is directly linked to six water molecules in the first hydration shell and the remaining three water molecules are linked through six hydrogen bonds in the second hydration shell. The difference in energy between the most stable structure and the least stable structure is 9.89 kcal/mol. The conformer with the 6 + 3 configuration is more stable than that with the 8 + 1 configuration, where the former has 6 hydrogen bonds

Table 1
Calculated values of different structural parameters and energies of $Sr^{2+}-nH_2O$ (n = 1–24) hydrated cluster at B3LYP level of theory using cc-PVDZ basis function for H and O and 3–21 G basis function for Sr.

Structures	No of isomers	Bond distance (Å)		No. of hydrogen bonds
		Minimum	Maximum	
$Sr^{2+}-H_2O$		2.5106		0
$Sr^{2+}-2H_2O$	2			
II-a		2.5470	2.5470	0
$Sr^{2+}-3H_2O$	3			
III-a		2.5302	2.5312	0
$Sr^{2+}-4H_2O$	5			
IV-a		2.5497	2.5505	0
$Sr^{2+}-5H_2O$	6			
V-a		2.5628	2.5923	0
$Sr^{2+}-6H_2O$	7			
VI-a		2.5923	2.5968	0
$Sr^{2+}-7H_2O$	5			
VII-a		2.5534	2.6325	2
$Sr^{2+}-8H_2O$	6			
VIII-a		2.5603	2.6180	4
$Sr^{2+}-9H_2O$	3			
IX-a		2.5665	2.5738	6
$Sr^{2+}-10H_2O$	2			
X-a		2.5560	2.5746	8
$Sr^{2+}-11H_2O$	3			
XI-a		2.5805	2.7954	5
$Sr^{2+}-12H_2O$	3			
XII-a		2.5668	2.8534	7
$Sr^{2+}-13H_2O$	1			
XIII		2.5801	2.8372	11
$Sr^{2+}-16H_2O$	1			
XVI		2.5660	2.8339	15
$Sr^{2+}-24H_2O$	1			
XXIV		2.5903	2.7687	31

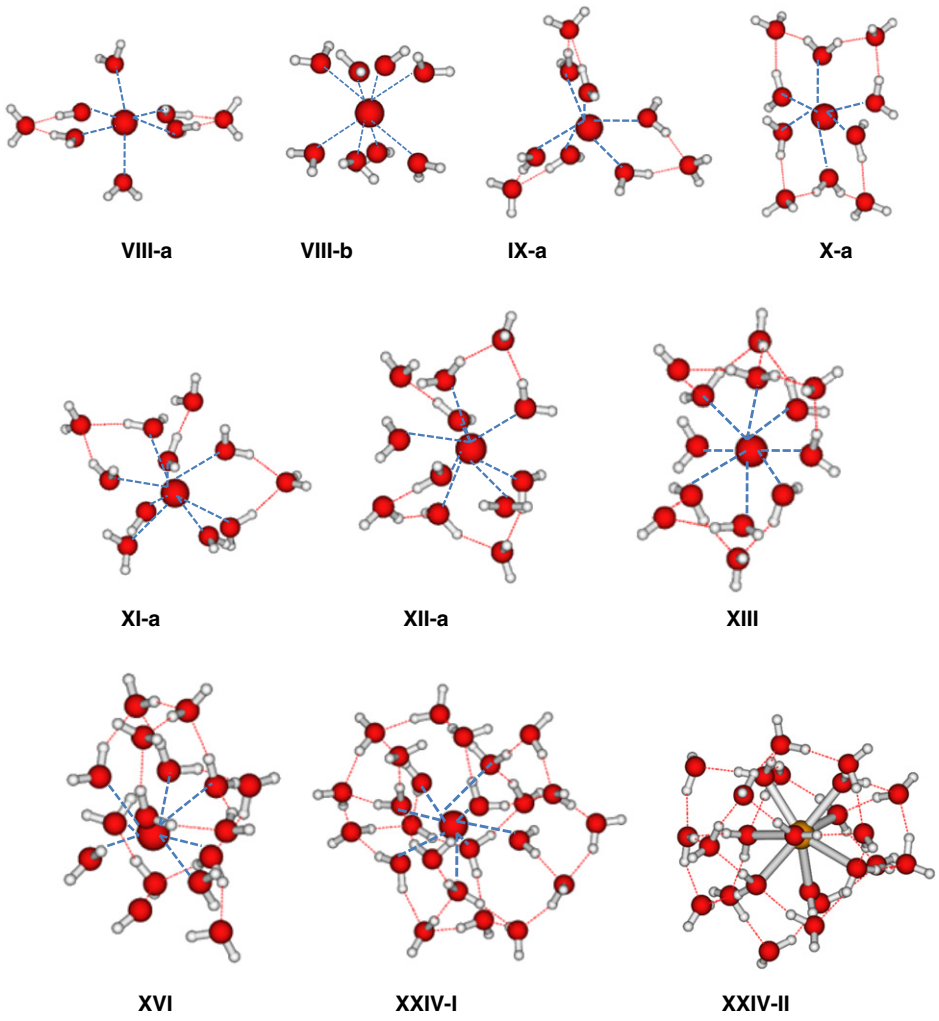

Fig. 1. Optimized minimum energy structure at B3LYP level of theory using ccPVDZ basis function for H and O and 3–21 G basis function for Sr for (VIII-a) $Sr^{2+}-8H_2O$, (IX-a) $Sr^{2+}-9H_2O$, (X-a) $Sr^{2+}-10H_2O$, (XI-a) $Sr^{2+}-11H_2O$, (XII-a) $Sr^{2+}-12H_2O$, (XIII) $Sr^{2+}-13H_2O$, (XVI) $Sr^{2+}-16H_2O$ and (XXIV) $Sr^{2+}-24H_2O$ hydrated clusters. The largest red spheres, medium sized red spheres and smallest gray spheres are represented by Sr atom, O atom and H atom, respectively. The thin line corresponds to hydrogen bonding and the thick dashed line corresponds to metal–oxygen (M–O) bond.

and the latter contains only 2 hydrogen bonds. In the case of the deca-hydrate $Sr^{2+}-(H_2O)_{10}$ cluster two minimum energy conformers were predicted. Among all of the predicted conformers, the structure labeled X-a in Fig. 1 is the most stable, where the Sr metal ion is directly linked to six water molecules in the first hydration shell and the remaining four water molecules are in the second hydration shell, linked through 8 hydrogen bonds, with a 6+4 configuration. The difference in energy between the most stable structure (X-a) and the least stable structure is 2.83 kcal/mol. The conformer with the 6+4 configuration is more stable than the 8+2 configuration, where the former has 8 hydrogen bonds and the latter has only 4 hydrogen bonds.

In the case of the adeka-hydrated $Sr^{2+}-(H_2O)_{11}$ cluster, three equilibrium conformers were confirmed. Among the various conformers, the structure of XI-a (Fig. 1) is the most stable, where the Sr metal ion is directly linked to eight water molecules in the first hydration shell and the remaining three water molecules are indirectly linked through 5 hydrogen bonds in the second hydration shell to generate a 6+5 configuration. The most stable structure (XI-a, Fig. 1) is 2.22 kcal/mol lower in energy than the least stable isomer. The isomer with the 8+3 configuration is more stable than the isomer with the 6+5 configuration, even though in this case, the former has 5 hydrogen bonds and the latter has 10 hydrogen bonds. The metal ion–water interaction in which there are 8 water molecules in the first solvation shell with 5 H-bonds is stronger than the metal ion–water interaction with 6 water molecules in the first solvation shell with 10 H-bonds. There is a competition between the direct metal ion–water interaction and water–water interaction through H bonding.

In the case of the dodeca-hydrate $Sr^{2+}-(H_2O)_{12}$ cluster, three minimum energy structures were predicted. The most stable structure has an 8+4 configuration, where the Sr metal ion is directly linked to eight water molecules in the first hydration shell and the remaining four water molecules are present in the second hydration shell, linked through 7 hydrogen bonds (XII-a, Fig. 1). The energy difference between the most and least stable structures is 3.57 kcal/mol.

To further evaluate the stability of higher-order hydrated clusters, the hydrated cluster with thirteen water molecules, $Sr^{2+}-(H_2O)_{13}$, was optimized as shown in Fig. 1, (XIII). Here also, we obtained a structure with eight water molecules in the first solvation shell in a distorted cubic arrangement with 5 second sphere water molecules connected by 11 hydrogen bonds to give an 8+5 configuration. The eight coordinate first solvation shell is maintained in the hydrated cluster even though the number of hydrogen bonds increased.

To further confirm the stability of the eight coordinate first solvation shell, larger hydrated clusters with sixteen and twenty four water molecules were also optimized. The optimized structures with sixteen and twenty four water molecules are displayed in Fig. 1 (XVI) and (XXIV). In the $Sr^{2+}-(H_2O)_{16}$ hydrated cluster, eight water molecules are directly

Table 2
Calculated values of different thermodynamic parameters of $Sr^{2+}-nH_2O$ (n = 1–24) hydrated cluster at B3LYP and MP2 levels of theory using cc-PVDZ basis function for H and O and 3–21 G basis function for Sr. All values are zero point and thermal energy corrected.

Structures	U^{int} (kcal/mol)	U^{hyd} (kcal/mol)	H^{int} (kcal/mol)	H^{hyd} (kcal/mol)	H_W^{hyd} (kcal/mol)	[a]U^{hyd} (kcal/mol)	[a]H^{hyd} (kcal/mol)
$Sr^{2+}-H_2O$ I	−43.70	−43.70	−44.30	−44.30	−44.30 (−48.09)	−39.46	−40.05
$Sr^{2+}-2H_2O$ II-a	−86.93	−84.72	−88.12	−85.91	−85.91 (−89.20)	−76.68	−77.86
$Sr^{2+}-3H_2O$ III-a	−126.40	−119.49	−128.17	−121.27	−121.04 (−123.64)	−110.94	−112.72
$Sr^{2+}-4H_2O$ IV-a	−165.74	−154.65	−168.11	−157.02	−156.15 (−153.31)	−141.98	−144.35
$Sr^{2+}-5H_2O$ V-a	−200.23	−184.71	−203.19	−187.68	−184.83 (−177.82)	−169.44	−172.4
$Sr^{2+}-6H_2O$ VI-a	−230.34	−213.13	−233.89	−216.69	−214.80 (−200.18)	−195.85	−199.4
$Sr^{2+}-7H_2O$ VII-a	−242.68	−232.90	−246.83	−237.05	−236.97	−214.55	−218.7
$Sr^{2+}-8H_2O$ VIII-a	−260.78	−254.23	−265.52	−258.97	−258.91	−233.66	−238.4
$Sr^{2+}-9H_2O$ IX-a	−283.08	−272.13	−288.42	−277.46	−277.42	−252.07	−257.4
$Sr^{2+}-10H_2O$ X-a	−300.20	−289.42	−306.12	−295.35	−295.22	−266.27	−272.19
$Sr^{2+}-11H_2O$ XI-a	−296.82	−299.61	−303.33	−306.13	−305.55	−279.58	−286.1
$Sr^{2+}-12H_2O$ XII-a	−324.89	−318.34	−332.00	−325.45	−325.37	−296.47	−303.58
$Sr^{2+}-13H_2O$ XIII	−318.38	−333.40	−326.09	−341.10	−341.10	−309.85	−317.55
$Sr^{2+}-16H_2O$ XVI	−331.58	−383.81	−341.06	−393.29	−393.29	−351.32	−360.80
$Sr^{2+}-24H_2O$ XXIV	−359.58	−499.26	−373.80	−513.48	−513.48		

Values in parenthesis are experimental enthalpy values.
[a] Calculated at MP2 level of theory.

coordinated to the Sr metal ion in a distorted cubic geometry comprising the first solvation shell and the remaining eight water molecules are linked through a fifteen hydrogen-bonded network in the second solvation shell with an 8 + 8 configuration. No water molecules were in the third solvation shell.

The $Sr^{2+}-(H_2O)_{24}$ hydrated cluster has a minimum energy configuration with eight water molecules coordinated to the Sr metal ion in a distorted cubic fashion in the first solvation shell, fifteen water molecules in the second solvation shell, and the remaining one water molecule is located in the third solvation shell, with a total of 31 hydrogen bonds and an overall 8 + 15 + 1 configuration.

The theoretically predicted coordination number of 8 for the first shell based on the QM optimized cluster structures is in agreement with the coordination number predicted by the XAFS method [33]. The present theoretical $Sr^{2+}-O$ bond distance (2.59 Å) is also in excellent agreement with the XAFS results of 2.60 Å [33]. The QM optimized structure of $Sr^{2+}-(H_2O)_{24}$ was further re-optimized using the conductor like screening solvation model (COSMO), implemented in the Turbomole package [84] at the B3LYP/TZVP level of theory, to take into account the bulk continuum solvent effect on the structure and CN. The optimized structure is presented in Fig. 1 (XXIV-II). Here, the first shell CN remains unchanged from the gas phase value of 8. The $Sr^{2+}-O$ distance is found to be 2.64 Å, which is very close to the experimentally reported value of 2.60 Å.

3.2. Interaction energy, hydration energy, and enthalpy

This section presents a discussion of the energy parameters, interaction energy (E^{int}) and hydration energy (E^{hyd}), which are the two most important energy parameters for the metal-ion clusters that are regularly discussed in the popular discrete solvent model. The zero point energy and thermally corrected values of the interaction energy (U^{int}) and hydration energy (U^{hyd}) of the $Sr^{2+}-(H_2O)_n$ cluster are given in Table 2 and Fig. 2, at both the B3LYP and MP2 levels of theory. The U^{int} curve assumes an almost constant value after ~10 H_2O units, which indicates that the metal ion does not interact with any further solvent water molecules that are added after the first ~10 units of H_2O molecules. However, the structure optimization presented in the previous section indicated that the first shell coordination number was 8 even in the presence of 10 or more water units, whereas an analysis of the energetics shows that interaction with the metal ion takes place with up to 10 water molecules. The latter is explained by the strong polarization of the doubly charged metal ion on the water molecules of the second solvation shell.

The calculated value of the hydration energy (U^{hyd}) of the cluster increases as the number of solvent water molecules increases, accounting for ion–solvent interaction as well as inter-solvent H-bonding interaction. The calculated values of U^{hyd} are plotted against the number of water molecules, n, in Fig. 2 by using the highest U^{hyd} value for a particular size of the hydrated cluster. It is to be noted that the most stable conformer for a hydrated $Sr^{2+}-(H_2O)_n$ cluster of a particular size has the highest U^{hyd}, as expected. The hydration energy and enthalpy were also calculated at the MP2 level of theory to evaluate the consistency with the DFT level of theory using the 3–21 G basis set for the Sr^{2+} metal ion. From Table 2, it can be seen that the calculated hydration energy was overestimated by only 4.3%–5.42% at the B3LYP level of density functional theory using the 3–21 G basis function for up to n = 24 water molecules, compared to the MP2 level of theory. In view of the high computational cost of the MP2 level of theory, this overestimation by the DFT method seems to be within acceptable limits.

The enthalpy of interaction (H^{int}) was also calculated for each conformer of the $Sr^{2+}-(H_2O)_n$ hydrated cluster, and the values are given in Fig. 2 and Table 2. The plot of the interaction enthalpy, H^{int}, against the number of water molecules, n, for the $Sr^{2+}-(H_2O)_n$ hydrated cluster is shown in Fig. 2. The interaction energy/enthalpy was

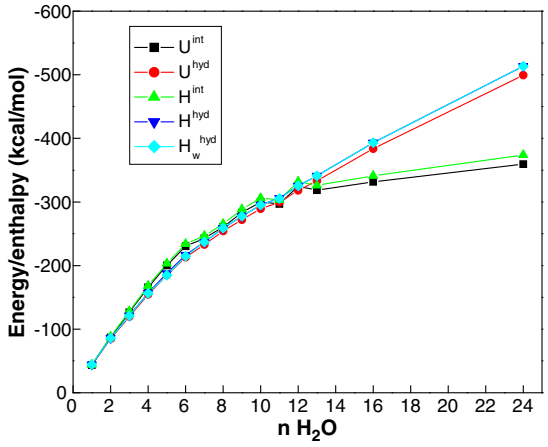

Fig. 2. U^{int}, U^{hyd}, H^{int}, H^{hyd}, and H_W^{hyd} versus number of water molecules in hydrated $Sr^{2+}-(H_2O)_n$, n = 1–24 cluster at the same level of theory as in Fig. 1. The values of U^{int}, U^{hyd}, H^{int} and H^{hyd} have been taken for the most stable structure of particular size of the cluster. The values of H_W^{hyd} are calculated based on population of different minimum energy structures. Population of different conformers is calculated based on free energy change at 298.15 K following Boltzmann distribution.

considered for the most stable conformer of a particular size of the hydrated cluster. It is interesting to note that for each hydrated $Sr^{2+}-(H_2O)_n$ cluster, the calculated H^{int} is at a maximum for a structure in which there is no inter-solvent H-bonding interaction up to n ~ 10. It is readily evident that there is a difference between U^{int}/H^{int} and U^{hyd}/H^{hyd} for clusters larger than n = 10. This is due to the fact that the interaction energy/enthalpy represents only the net binding energy/enthalpy of the metal ion with the solvent $(H_2O)_n$ cluster unit. Thus, the value of U^{int}/H^{int} for the hydrated $Sr^{2+}-(H_2O)_n$ clusters increases as long as the individual solvent molecules bind directly to the metal ion in a largely independent manner. However, the U^{hyd}/H^{hyd} energies represent the total interaction energy/enthalpy of the metal ion with n individual solvent water molecules and the energy due to inter-solvent interaction among these n H_2O molecules. Thus, U^{hyd} for the hydrated $Sr^{2+}-(H_2O)_n$ clusters increases consistently with an increase in the number of solvent water molecules. From the figure, it is seen that there is a large difference between U^{int} and U^{hyd} for larger clusters. This is due to the effect of hydrogen bonding among the water molecules. From the figure, it is also clear that the U^{int}/H^{int} plots assume an almost constant value after ~10 water molecules whereas the U^{hyd} increases continuously with the addition of water molecules, attributed to the increase in the hydration energy due to increased hydrogen bonding. The weighted averaged hydration enthalpies (H_W^{hyd}) were also evaluated with the successive increase of water molecules and these relationships are also plotted in Fig. 2. There are no major changes in the hydration enthalpies due to the statistical averaging of various conformers. The weighted average values were calculated based on the population of different minimum energy structures. The population of various conformers was calculated based on the free energy change at 298.15 K following the Boltzmann distribution.

The hydration energy and enthalpy were also calculated at the MP2 level of theory to verify the accuracy of the DFT level of theory, by using the extended LANL2DZ basis set for the Sr metal ion. To further assess the effect of the basis set of the Sr^{2+} metal ion on the energetics, the extended ECP-based LANL2DZ basis set was also applied for Sr instead of the 3–21 G basis set, and the calculated results for the hydration energy up to n = 6 water molecules are given in the Supplementary information, Table S1. Though the change in the basis set lowers the hydration energy by 0.16–2.33 kcal/mol in the B3LYP level of calculation, the change is insignificant in the case of the MP2 level of theory. Thus, the use of the 3–21 G basis set for Sr appears to be reasonable. The hydration enthalpy calculated using the 3–21 G basis set is also reported in Table S1, along with experimental results from literature [23]. The calculated value was underestimated at the DFT level of theory for up to n = 4 water molecules, after which the hydration enthalpy was overestimated. The calculated hydration enthalpy value at the DFT level of theory was very close to the experimental value up to n = 5 water molecules (see Table 2), but is overestimated by 12.39 kcal/mol (5.82%) compared to the experimental results for n = 6 water molecules. Using the MP2 level of theory, the calculated results for the hydration enthalpy were underestimated compared to the experimental results up to n = 5 water molecules, but was in excellent agreement with the experimental result for n = 6 water molecules. The values for the hydration enthalpy calculated at the MP2/6–31 + G* level of theory by Feller et al. [56] are also presented in Table S1. Even though the results presented in that study for up to n = 3 water molecules matched quite well with the experimental results, the deviation after n = 3 water molecules was quite significant, and the performance was even poorer than the DFT predicted results. The use of a mixed basis set by using the LANL2DZ ECP basis set has been previously applied for various metal ions [85–87]. To study the effect of the mixed basis set, we performed the standard BSSE calculation [88]. The BSSE corrected results are tabulated in the supplementary Table S2. The interaction energy (E^{int}) and hydration energy (E^{hyd}) were lowered by 9%–10% at both the DFT and MP2 levels of theory after the BSSE correction. The interaction enthalpy and hydration enthalpy for higher hydrated clusters with n > 6 were also calculated and were already discussed. From the results, it was observed that for clusters with more than n = 10 water molecules, the increment in the interaction enthalpy was slowed, whereas a linear increase was observed for the hydration enthalpy. Though the hydration enthalpy increased linearly, the successive hydration enthalpy increment per water molecule gradually decreased. The optimized coordinates of the hydrated cluster can be supplied on request.

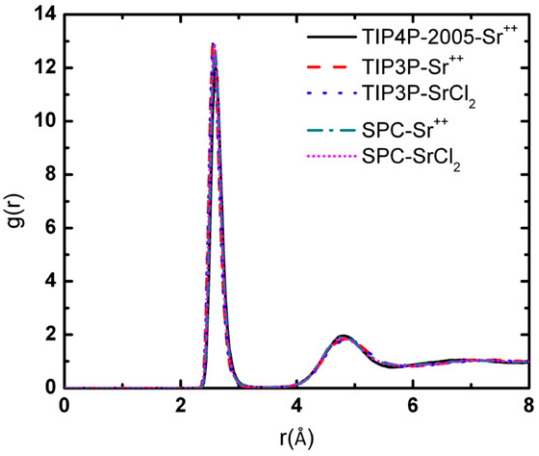

Fig. 3. Radial distribution function of $Sr^{2+}-O$ for various different water models.

3.3. Hydration structure and coordination number from MD

The coordination numbers of the first and second shell of the Sr^{2+} ion were predicted to be 8 and 15 based on quantum electronic structure calculation. As a counter check, the classical MD simulations were also evaluated. It is to be noted that various models for water are available. The MD results are given in Table 3, and the radial distribution functions (RDF) for the Sr^{2+} ion with respect to the oxygen atom of various water models are presented in Fig. 3. The RDF is used to calculate the CN for the first solvation shell. The average CN can be calculated by integrating the RDF with respect to distance from the metal ion. Integrating the RDF up to the first minimum yields the CN for the first solvation shell. Fig. 4 shows the running value of the CN with distance. The various models yield CN values in the range of 8.2–8.28. This strongly indicates a very high probability of a CN ~ 8 for the first coordination shell of Sr^{2+}. This is also corroborated by the stronger peak at 8 in the CN distribution as shown in the

Table 3
First maximum/minimum and second maximum/minimum of radial distribution functions (Sr – O) and coordination numbers of different water models using molecular dynamics.

Water models	First max r(Å)	First min r(Å)	Second max r(Å)	Second min r(Å)	Coordination number (1st shell)	Coordination number (2nd shell)
TIP4P-2005	2.58	3.46	4.82	5.62	8.24	19
TIP3P	2.55	3.46	4.82	5.92	8.24	22.7
TIP3P + $2Cl^-$	2.55	3.42	4.85	5.95	8.28	22.7
SPC	2.58	3.39	4.78	5.81	8.20	21.1
SPC + $2Cl^-$	2.58	3.42	4.78	5.88	8.28	21.7

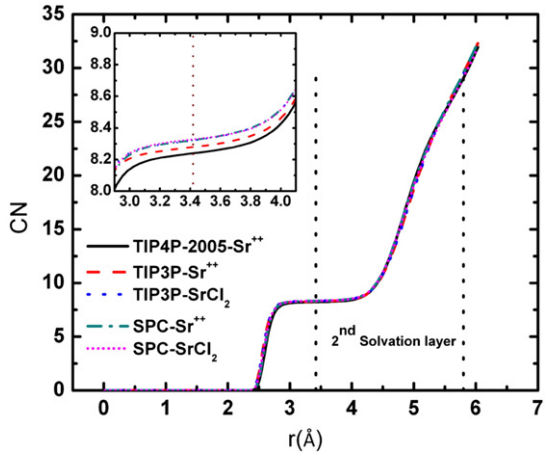

Fig. 4. CN as a function of radial distance for different water models.

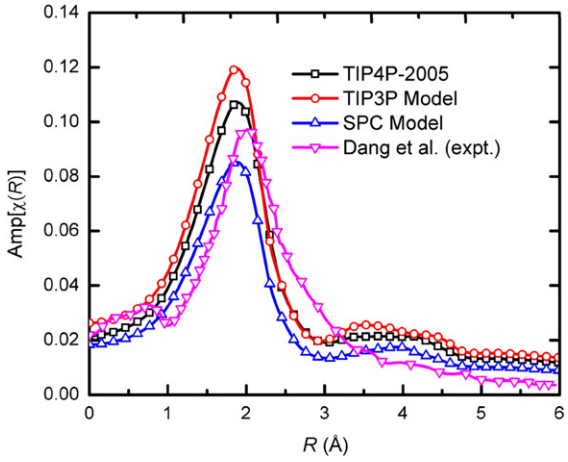

Fig. 6. Comparison of MD–EXAFS spectra with experimental EXAFS spectrum for Sr^{2+} – O in water.

Supplementary Fig. S2. These results are in good agreement with previous reports [40,89–91]. The average value of the CN for the second shell was found to be 21. However, the TIP4P-2005 model yields the lowest CN for the second shell of ~19, which is the closest to the value predicted from the quantum mechanical approach.

We also performed the MD–EXAFS study on the Sr^{2+} – SPC/E water system. Although the results of this model are not reported in this paper, the calculated RDF and k^3-weighted $\chi(k)$ are in excellent agreement with the results reported by Palmer et al. [39]. Subsequently, this approach was extended to other water models viz., SPC, TIP3P, and TIP4P-2005. The calculated results are presented in Figs. 5 and 6. The noise level of the EXAFS spectra in k-space was unacceptably high. Hence, to minimize the noise, various k^n-weighted $\chi(k)$ data (n = 1, 2, 3) were examined, and the calculated $k^3\chi(k)$ data was used to illustrate the behavior of the various water models. The results obtained using the TIP4P-2005 model were in good agreement with the results reported by Palmer et al., in contrast to the other two models. The Fourier transformed data of $k^3\chi(k)$ were used to obtain the uncorrected local structure factor, which was considered to be duplication of the EXAFS spectra. The accuracy of the theoretical structure factor was limited because of sinusoidal oscillations of all paths and associated phase shift variations during the conversion from k-space to R-space. The MD–EXAFS (amplitude of $\chi(R)$ without weighting) spectra for different water models were compared with the experimental data of Dang et al. [46]. The MD–EXAFS spectra were found to have a mean phase lead of 0.104 Å over the actual value [46] of 1.986 Å (experimental prediction [33] 1.93 Å). In addition, relative to the experimental results, various amplitudes were observed with the different classical water models; these values are tabulated in Table 4. This behavior was expected given that all classical models neglect the polarizability of water. From the MD–EXAFS spectra and coordination number analysis of the first and second hydration shells of Sr^{2+}, it was observed that the water potential of the TIP4P-2005 model is superior to the water potentials of the other models for the Sr ion–water systems.

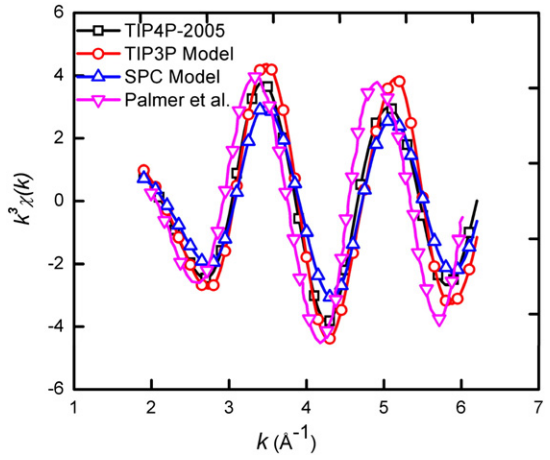

Fig. 5. Comparison of $k^3\chi(k)$ with respect to wave vector (k) for Sr^{2+} – O for different water models.

4. Conclusion

In the present study, the $Sr^{2+}-(H_2O)_n$ (n = 1–24) cluster system was investigated using hybrid DFT functional (B3LYP) and ab initio MP2 levels of theory by employing the cc-PVDZ basis function for H and O, and a split valence 3–21 G and the extended LANL2DZ basis functions for Sr. Notably, the U^{int}/H^{int} curve was found to assume a relatively constant value after ~10 H_2O units indicating that the polarization effect of the Sr^{2+} metal ion on the water molecules of the second solvation shell is considerably reduced after n ~ 10 water molecules. The inner-sphere coordination number of the hydrated clusters with n = 11 to 24 water units was found to be 8 based on the optimized structures, with m2 and m3 water molecules in the second and third solvation shells, in a 8 + m2 + m3 configuration (here, m2 = 3, 4, 5, 8, 15 and m3 = 1). The geometrically predicted first shell coordination number of 8 is in quantitative agreement with the coordination number predicted by the XAFS method [32]. The theoretical Sr^{2+} – O bond distance of 2.59 Å predicted from the simulations presented herein is also in excellent agreement with the XAFS results of 2.60 Å [32]. The calculated interaction energy/enthalpy profiles show flattening at n ~ 10, whereas the hydration energy increases with the addition of successive solvent H_2O molecules in the hydrated cluster, $Sr^{2+}-(H_2O)_n$ (n = 1–24). The coordination number and Sr^{2+} – O bond distance were further re-confirmed using the COSMO solvation model at the B3LYP/TZVP level of theory, and classical MD simulations were also performed for various water models. The Sr^{2+} coordination number was observed to be between 8 and 9 using the different models.

Table 4
The MD–EXAFS spectra comparison with respect to first maximum peak location, phase lead and amplitudes for various water models with respect to the experimental spectrum.

Water model	First maximum peak (Å)	Phase lead (Å)	Amplitude (Å)
SPC model	1.872	0.114	0.0850
TIP3P model	1.872	0.104	0.1196
TIP4P-2005	1.902	0.084	0.1071
Experiment	1.986	–	0.0968

Based on the MD–EXAFS spectra and coordination number analyses for first and second shells, the TIP4P-2005 water model was found to provide good agreement with the experimental EXAFS spectrum in comparison with the other classical water models, though there was a slight deviation in the estimation of the coordination number with this model. The present work is anticipated to stimulate further experimental studies, as well as facilitate modeling of the separation of strontium ions from various forms of chemical and radioactive wastes.

Acknowledgments

This work was supported by the Bhabha Atomic Research Centre (BARC) — BNRS, Government of India (Grant No. 2008/36/105-BRNS/4036).

Appendix A. Supplementary data

Supplementary data to this article can be found online at http://dx.doi.org/10.1016/j.molliq.2012.05.006.

References

[1] M.K. Beyer, Mass Spectrometry Review 26 (2007) 517–541.
[2] J.M. Lisy, International Review in Physical Chemistry 16 (1997) 267–289.
[3] V.E. Bondybey, M.K. Beyer, International Review in Physical Chemistry 21 (2002) 277–306.
[4] K.H. Michaellian, M. Moskovits, Nature 273 (1978) 135–136.
[5] R.W. Impey, P.A. Madden, I.R. McDonald, Journal of Physical Chemistry 87 (1983) 5071–5083.
[6] L.X. Dang, J.E. Rice, J. Caldwell, P.A. Kollman, Journal of the American Chemical Society 113 (1991) 2481–2486.
[7] L.X. Dang, Journal of Chemical Physics 96 (1992) 6970–6977.
[8] H. Ohtaki, T. Radnai, Chemical Reviews 93 (1993) 1157–1204.
[9] R.N. Barnett, U. Landman, Physical Review Letter 70 (1993) 1775–1778.
[10] D. Feller, E.D. Glendening, R.A. Kendall, K.A. Peterson, Journal of Chemical Physics 100 (1994) 4981–4997.
[11] D.A. Doyle, J.M. Cabral, R.A. Pfuetzner, A.L. Gulbis, S.L. Cohen, B.T. Chait, R. MacKinnon, Science 280 (1998) 69–77.
[12] K. Hashimoto, T. Kamimoto, (n = 1−6 and 8), Journal of the American Chemical Society 120 (1998) 3560–3570.
[13] A.K. Pathak, T. Mukherjee, D.K. Maity, Journal of Chemical Physics 124 (2006) (024322-024322-7).
[14] S.M. Ali, S. De, D.K. Maity, Journal of Chemical Physics 127 (2007) (044303-044303-11).
[15] S. De, S.M. Ali, A. Ali, V.G. Gaikar, Physical Chemistry Chemical Physics 11 (2009) 8285–8294.
[16] C.M. Whitehouse, R.N. Dreyer, M. Yamashita, J.B. Fenn, Analytical Chemistry 57 (1985) 675–679.
[17] M. Yamashita, J.B. Fenn, Journal of Physical Chemistry 88 (1984) 4451–4459.
[18] M. Peschke, A.T. Blades, P. Kebarle, Journal of Physical Chemistry A 102 (1998) 9978–9985.
[19] A.T. Blades, P. Jayaweera, M.G. Ikonomou, P. Kebarle, Journal of Chemical Physics 92 (1990) 5900–5906.
[20] S.E. Rodriguez-Cruz, R.A. Jockusch, E.R. Williams, Journal of the American Chemical Society 121 (1999) 8898–8906.
[21] R.L. Wong, K. Paech, E.R. Williams, International Journal of Mass Spectrometry 232 (2004) 59–66.
[22] D.R. Carl, R.M. Moision, P.B. Armentrout, (x = 5–9), International Journal of Mass Spectrometry 265 (2007) 308–325.
[23] D.R. Carl, B.K. Chatterjee, P.B. Armentrout, Journal of Chemical Physics 132 (2010) (044303-044303-12).
[24] I. Dzidic, P. Kebarle, Journal of Physical Chemistry 74 (1970) 1466–1474.
[25] N.F. Dalleska, K. Honma, L.S. Sunderlin, P.B. Armentrout, Journal of the American Chemical Society 116 (1994) 3519–3528.
[26] J.W. Shin, N.I. Hammer, E.G. Diken, M.A. Johnson, R.S. Walters, T.D. Jaeger, M.A. Duncan, R.A. Christie, K.D. Jordan, Science 304 (2004) 1137–1140.
[27] P. D'Angelo, H.F. Nolting, N.V. Pavel, Physical Review A 53 (1996) 798–895.
[28] G.W. Neilson, R.D. Broadbent, Chemical Physics Letter 167 (1990) 429–431.
[29] R.H. Parkman, J.M. Charnock, F.R. Livens, D.J. Vaughan, Geochimica et Cosmochimica Acta 62 (1998) 1481–1492.
[30] I. Persson, M. Sandstrom, H. Yokoyama, M. Chaudhry, Zeitschrift fur Naturforschung A: Journal of Physical Sciences 50a (1995) 21–37.
[31] T.M. Stewards, C.M.B. Henderson, J.M. Charnock, T. Driesner, Geochimica et Cosmochimica Acta 63 (1999) 2409–2418.
[32] G. Moreau, L. Helm, J. Purans, A.E. Merbach, Journal of Physical Chemistry A 106 (2002) 3034–3043.
[33] D.M. Pfund, J.G. Darab, J.L. Fulton, Y. Ma, Journal of Physical Chemistry 98 (1994) 13102–13107.
[34] S. Ramos, G.W. Neilson, A.C. Barnes, M.J. Capita'n, Journal of Chemical Physics 118 (2003) 5542–5546.
[35] R. Caminiti, A. Musinu, G. Paschina, G. Pinna, Journal of Applied Crystallography 15 (1982) 482–487.
[36] L. Axe, G.B. Bunker, P.R. Anderson, T.A. Tyson, Journal of Colloid and Interface Science 199 (1998) 44–52.
[37] P.A. O'Day, M. Newvillre, P.S. Neuhoff, N. Sahai, S.A. Carroll, Journal of Colloid and Interface Science 222 (2000) 184–197.
[38] N. Sahai, S.A. Carroll, S. Roberts, P.A. O'Day, Journal of Colloid and Interface Science 222 (2000) 198–212.
[39] B.J. Palmer, D.M. Pfund, J.L. Fulton, Journal of Physical Chemistry 100 (1996) 13393–13398.
[40] E. Spohr, G. Pilinkis, K. Heinzinger, P. Bopp, M.M. Probst, Journal of Physical Chemistry 92 (1988) 6754–6761.
[41] D.J. Harris, J.P. Brodholt, D.M. Sherman, The Journal of Physical Chemistry B 107 (2003) 9056–9058.
[42] T.S. Hofer, B.R. Randolf, B.M. Rode, The Journal of Physical Chemistry B 110 (2006) 20409–20417.
[43] J.M. Martinez, R.R. Pappalardo, E.S. Marcos, K. Refson, S. Diaz-Moreno, A. Munoz-PÃ¡ez, The Journal of Physical Chemistry B 102 (1998) 3272–3282.
[44] B.K. Teo, EXAFS: Basic Principles and Data Analysis, Springer-Verlag, Berlin, 1986.
[45] J.L. Fulton, S.M. Heald, Y.S. Badyal, J.M. Simonson, Journal of Physical Chemistry A 107 (2003) 4688–4696.
[46] L.X. Dang, G.K. Schenter, J.L. Fulton, The Journal of Physical Chemistry B 107 (2003) 14119–14123.
[47] V.A. Glezakou, Y. Chen, J. Fulton, G. Schenter, L. Dang, Theoretica Chimica Acta 115 (2006) 86–99.
[48] L.X. Dang, G.K. Schenter, V.A. Glezakou, J.L. Fulton, The Journal of Physical Chemistry B 110 (2006) 23644–23654.
[49] L.A. LaJohn, P.A. Christiansen, R.B. Roos, T. Atashroo, W.C. Ermler, Journal of Chemical Physics 87 (1987) 2812–2824.
[50] C.W. Bauschlicher, S.R. Langhoff, H. Partridge, J.E. Rice, A. Komornicki, (n = 1–4), Journal of Chemical Physics 95 (1991) 5142–5148.
[51] C.W. Bauschlicher, M. Sodupe, H. Partridge, Journal of Chemical Physics 96 (1992) 4453–4463.
[52] C.J. Burnham, M.K. Petersen, T.J.F. Day, S.S. Iyengar, G.A. Voth, Journal of Chemical Physics 124 (2006) (024327-024327-9).
[53] D. Feller, Journal of Physical Chemistry A 101 (1997) 2723–2731.
[54] D. Feller, E.D. Glendening, D.E. Woon, M.W. Feyereisen, Journal of Chemical Physics 103 (1995) 3526–3542.
[55] E.D. Glendening, D. Feller, Journal of Physical Chemistry 99 (1995) 3060–3067.
[56] E.D. Glendening, D. Feller, Journal of Physical Chemistry 100 (1996) 4790–4797.
[57] E.D. Glendening, D. Feller, M.A. Thompson, Journal of the American Chemical Society 116 (1994) 10657–10669.
[58] W.L. Jorgensen, D.L. Severance, Journal of Chemical Physics 99 (1993) 4233–4235.
[59] M. Kaupp, P.V. Schleyer, Journal of Physical Chemistry 96 (1992) 7316–7323.
[60] M. Klobukowski, Canadian Journal of Chemistry 70 (1992) 589–595.
[61] M. Kołaski, H.M. Lee, Y.C. Choi, K.S. Kim, P. Tarakeshwar, D.J. Miller, J.M. Lisy, Journal of Chemical Physics 126 (2007) (074302-074302-11).
[62] D.J. Miller, J.M. Lisy, Journal of Chemical Physics 124 (2006) (024319-024319-9).
[63] A.C. Olleta, H.M. Lee, K.S. Kim, Journal of Chemical Physics 124 (2006) (024321-024321-13).
[64] L.M. Ramaniah, M. Bernasconi, M. Parrinello, Journal of Chemical Physics 111 (1999) 1587–1591.
[65] J.L.F. Abascal, C. Vega, Journal of Chemical Physics 123 (2005) (234505-234505-12).
[66] H.J.C. Berendsen, J.R. Grigera, T.P. Straatsma, Journal of Physical Chemistry 91 (1987) 6269–6271.
[67] H.J.C. Berendsen, J.P.M. Postma, W.Fv. Gunsteren, J. Hermans, in: D.B. Pullman (Ed.), Intermolecular Forces, Reidel, 1981, p. 331.
[68] W.L. Jorgensen, J. Chandrasekhar, J.D. Madura, R.W. Impey, M.L. Klein, Journal of Chemical Physics 79 (1983) 926–935.
[69] C. Vega, E. Sanz, J.L.F. Abascal, Journal of Chemical Physics 122 (2005) (114507-114507-9).
[70] Y. Wu, H.L. Tepper, G.A. Voth, Journal of Chemical Physics 124 (2006) (024503-0243503-12).
[71] J. Zielkiewicz, Journal of Chemical Physics 123 (2005) (104501-104501-6).
[72] A.D. Becke, Journal of Chemical Physics 98 (1998) 5648–5652.
[73] C. Lee, W. Yang, R.G. Parr, Physical Review B 37 (1988) 785–789.
[74] C. Moller, M.S. Plesset, Physical Review 46 (1934) 618–622.
[75] M.W. Schmidt, K.K. Baldridge, J.A. Boatz, Steven T. Elbert, M.S. Gordon, J.H. Jensen, S. Koseki, N. Matsunaga, K.A. Nguyen, S. Su, T.L. Windus, M. Dupuis, J.A. Montgomery, Journal of Computational Chemistry 14 (1993) 1347–1363.
[76] G. Schaftenaar, J.M. Noordik, Journal of Computer-Aided Molecular Design 14 (2000) 123–134.
[77] M.A. Scotto, G. Mallet, D. Vasilescu, Journal of Molecular Structure (THEOCHEM) 728 (2005) 231–242.
[78] S. Plimpton, Journal of Computational Physics 117 (1995) 1–19.
[79] S.I. Zabinsky, J.J. Rehr, A. Ankudinov, R.C. Albers, M.J. Eller, Physical Review B 52 (1995) 2995–3009.
[80] M. Newville, B. Ravel, D. Haskel, J.J. Rehr, E.A. Stern, Y. Yacoby, Physica B: Condensed Matter 208 (1995) 154–156.
[81] B. Ravel, M. Newville, Journal of Synchrotron Radiation 12 (2005) 537–541.
[82] M. Newville, Journal of Synchrotron Radiation 8 (2001) 322–324.
[83] M. Newville, FEFFIT Using FEFF to model XAFS Data, University of Chicago, Chicago, 1998.

[84] R. Ahlrichs, M. Bär, M. Häser, H. Horn, C. Kölmel, Chemical Physics Letter 162 (1989) 165–169.
[85] C.B. Messner, T.S. Hofer, B.R. Randolf, B.M. Rode, Chemical Physics Letter 501 (2011) 292–295.
[86] C.B. Messner, T.S. Hofer, B.R. Randolf, B.M. Rode, Physical Chemistry Chemical Physics 13 (2011) 224–229.
[87] A. Eizaguirre, O. Mó, M. Yáñez, J.Y. Salpin, Physical Chemistry Chemical Physics 13 (2011) 18409–18417.
[88] S.F. Boys, F. Bernardi, Molecular Physics 19 (1970) 553–566.
[89] D.E. Smith, L.X. Dang, Chemical Physics Letter 230 (1994) 209–214.
[90] H.S. Kim, Physical Chemistry Chemical Physics 2 (2000) 2919–2923.
[91] J.P. Larentzos, L.J. Criscenti, The Journal of Physical Chemistry B 112 (2008) 14243–14250.